Salt Llobregat, JJ.; Sala Piqueras, A. (2014). A new algorithm for dual-rate systems frequency response computation in discrete control systems. Applied Mathematical Modelling. 38(23):5692-5704. doi:10.1016/j.apm.2014.04.054.

A new Algorithm for Dual-Rate Systems Frequency Response Computation in discrete control systems

Julian Salt[1], Antonio Sala

Systems Eng. and Control Dept., Instituto de Automatica e Informatica Industrial, Universitat Politecnica de Valencia, Cno. Vera, s/n, E-46022 VALENCIA, SPAIN.
e-mail: {julian,asala}@isa.upv.es

Abstract

This paper addresses an easy computation of the multiple components of the response to a sinusoidal input of a dual-rate linear time-invariant discrete system from the Bode diagram of LTI systems arising from a lifted representation. Based on those results, a generalized Bode diagram is suggested. Some new conclusions derived from this conceptual interpretation are introduced. This diagram provides a better insight in the frequency-response issues in multivariable control than the standard Singular Value Decomposition of the lifted model. As an application, the output ripple suppression in a multirate control scheme is presented.

Keywords: Dual-rate systems, frequency response, digital control, Bode diagram

1. Motivation

The consideration of multirate systems (MRS) in fields like signal processing and communications are well established many years ago. Digital control is also an environment where multirate systems are used either to overcome practical difficulties or to achieve unattainable results by single rate control [1, 2, 3, 4]. In fact Dual-rate systems in systems and control have long ago been of interest to engineers [5]: low-latency measurements, limited-speed actuators in control loops, fast sensing in order to better filter

[1]At the time of first submission, J. Salt was on leave as visiting scholar at Department of Mechanical Engineering, Universiy of California at Berkeley. USA.

measurement noise, network load [6, 7], computational resources [8], zero-assignment [9], *etc.* are issues concerning possible applications advantages of dual-rate systems.

Although there are some techniques described in [10, 11, 12, 13], the usual procedure to handle a MRS that is a time-variable system is to consider the technique known as lifting (in control area) [14, 15, 16, 17] or blocking (in signal processing) [18]. With this procedure the system is transformed into a LTI system once the system description is enlarged over a "metaperiod". Using this technique, even from a single-input single-output (SISO) system an artificial multi-input and multi-output (MIMO) system is obtained.

One of the classical problems in multirate control is derived from the consideration that such MIMO lifted system can be controlled as any other multivariable MIMO one. However, there are not different input and output variables, but just one input and one output, "lifted" at different input and output sampling times in a periodically-repeating metaperiod. In automatic control field this procedure was originally denoted as Vectorial Switch Decomposition by Kranc [19]. Different authors proved that lifting and blocking were actually the exact same operation providing an unified analysis with that of periodic systems [20, 21]. Together to on-line identification of this kind of systems [22, 23, 24, 25], one of the recurrent topics that has been explored in this environment is the frequency response and its use in control [26, 27]. Indeed, frequency-response issues are still a current matter of interest in control [28, 29] and estimation problems [25].

From the above-presented considerations, it is common to study the frequency response of dual-rate plants by using singular value decomposition (SVD) of the lifted MIMO system. The conclusions are correct, but the results are partial due to the fact that the frequency response is obtained up to a metaperiod and lifting is disregarded. Hence, some relevant aspects for control cannot be obtained, as the single-rate lifted SVD leaves out some specific properties of the dual-rate setup.

An alternative approach is the lifting in "frequency" instead of the lifting in "time" that the above literature proposed. This is the so-called AC (alias component) matrix [30]. It is difficult and laborious to do this operation. Actually it is a hard task and for this reason it motivated contributions like [31] where a coprime periods were supposed in the dual-rate scheme.

Computation of the frequency response of non-conventionally-sampled systems was addressed in, for instance, [32, 33]. In [33], the goal was to detect ripples in the controlled variables as well as to generalize engineering-related

design criteria; the dual-rate frequency response to a sinusoidal input was be evaluated by checking the "conventional" Bode diagram of a particular discrete transfer function. However, the results only applied to the case when input sampling period T_u was an integer multiple or divisor of the output one T_y. This work will introduce a "generalized Bode diagram" which lifts such restriction, and includes several harmonic frequency components.

Preliminary work by the authors in [34] is extended in this contribution. A basic formula was introduced to easily obtain the multiple sinusoidal components of the dual-rate system's exact frequency response, under the assumption that the input and output periods were rationally related.

In the work here presented, the results are completed introducing a table of frequency components with an arrangement based on Bezout identity. Also, a generalised Bode diagram valid for coprime input/output periods is presented: the several harmonic components of a dual-rate response can be read as interleaved fragments of the frequency response of a particular single-rate system. Importantly, apart from a first academic example, the results are applied to feedback control systems, proposing a methodology to analyse the frequent output-ripple phenomena, allowing to overcome this anomalous performance which is not clearly detected from the SVD diagrams of the frequency response of the lifted system from previous literature.

The structure of the paper is as follows: next section recalls some preliminary material and founds definitions and notation; Section 3 presents the main result on frequencial components of the output of a dual-rate system; some numerical examples are explained in Section 4, and then in section 5 we will show the advantages of this new tool in a dual-rate control scheme analysis example where ripple effect appears and it is exactly detected by this computation tool. A conclusion section closes the paper.

2. Preliminaries and notation

Let us consider the transfer function $G(z) = B(z)/A(z)$, in the Z-transformed input-output domain representing a single-rate discrete-time linear time-invariant (LTI) system. When the above system is excited by an input $u(k) = a^k$, where a is *not* a pole of the system, the response admits a particular solution $y(k) = G(a)a^k$, because there exists a polynomial $S(z)$ such that the Z-transform of the output can be expressed as:

$$y(z) = G(z)u(z) = \frac{B(z)z}{A(z)(z-a)} = \frac{zG(a)}{z-a} + \frac{S(z)}{A(z)}$$

In the same way, when the input is $u(k) = e^{j\omega T_u k}$, such particular solution is $G(e^{j\omega T_u})e^{j\omega T_u k}$, usually denoted as frequency response, and the stationary response to sinusoidal signals can be easily determined from it by taking real and imaginary parts. The scalar T_u may be interpreted as "input sampling period". Of course, the actual computation of that solution does only have sense for stable systems or systems stabilized in closed loop.

A dual-rate discrete LTI system is one in which the input and output sequences are assumed to have different sampling periods, T_u and T_y. If they are rationaly related, it is possible to define the least common multiple $T_0 = lcm(T_u, T_y)$ usually known as "metaperiod" or "frame period" and there exist integers N_u, N_y such that $T_0 = T_u N_u = T_y N_y$ (indeed, then $T_u/T_y = N_y/N_u$ is a rational number). It is usual to define the "greatest common divisor sampling period" $T = gcd(T_u, T_y)$ as well, such that $T_0 = NT$ being $N = lcm(N_u, N_y)$; therefore $T_0 = NT = N_u T_u = N_y T_y$. With these conditions, the behaviour of the dual-rate system may be characterised via a "lifted" transfer function matrix:

$$y_l(z^N) = G_{lifted}(z^N) u_l(z^N) \tag{1}$$

where the variable z^N stands for the LTI z-transform argument at sampling period T_0, y_l is a vector of length N_y, u_l is a vector of length N_u and G_{lifted} is a $N_y \times N_u$ transfer function matrix [15]. The lengths of the vectors are increased in the case of MIMO systems (multiplied by the number of outputs and inputs, respectively). For convenience, zero-based array element count will be used in the sequel. For instance, the original T_y-sequence $y(k)$ and its lifted one $y_l(k)$ (T_0 related) are built in such a way that the i-th element of $y_l(k)$, to be denoted as $y_{l,i}(k)$, is $y(k * N + i)$, with $i = 0, N_u \ldots, N_u(N_y - 1)$.

In order to recover original sequences from lifted results in the Z-transformed domain, an expand operator [35] may be used, sometimes padding with zeros the intermediate samples.

Sampled-data lifted systems

If a strictly proper continuous system is discretised (assuming ZOH) at period T, with a realization $(A, B, C, 0)$, then the lifted dual-rate model has a realization (A_l, B_l, C_l, D_l), at period NT, where these matrices are obtained by repeated evaluations of the equations at sampling period T giving rise to

well-known convolution-like formulae. For instance:

$$y(kN+v) = Cx(kN+v) = C(A^v x(kN) + A^{v-1}Bu(kN) + \\ + A^{v-2}Bu(kN+1) + \ldots + Bu(kN+(v-1))) \quad (2)$$

for $v = 0, \ldots, N-1$, i.e., $y_{l,i}(kN) = y(kN+i)$. However, the zero-order-hold entails $u(kN+dN_y) = u(kN+(dN_y+1)) = \cdots = u(kN+(d+1)N_y-1) = u_{l,d}(kN)$ for all $d = 0, 1 \ldots, (N_u-1)$, where $u_{l,d}(kN)$ denotes each of the distinct control actions in a metaperiod. Therefore the lifted matrices are obtained by suitably stacking the results from the above equation. The reader is referred for details, omitted here for brevity, to [15, 17, 36].

Let us also recall the following complex exponential formula for later use: sequence t_k consisting on 1 for elements $k = 0, R, 2R, \ldots$ and zero for the rest can be described by:

$$t_k = \frac{1}{R} \sum_{l=0}^{R-1} e^{j2\pi lk/R} \quad (3)$$

By delaying such sequence, expressed as t_{k-s}, the sequence with ones at positions $s, R+s, 2R+s, \ldots$ and zeros elsewhere is also described.

3. Computation of frequency response

The purpose of this section is to introduce the calculation of the frequency response of a dual-rate discrete system when a lifted LTI representation of it (1) is available. It is assumed that the discrete-time input is the complex exponential sequence $e^{j\omega T_u k}$ and the output sampling period is T_y.

In many works in literature, the discrete frequency response operator for a given system is defined as the result of substituting $z = e^{j\omega T_0}$ in its equivalent discrete lifting operator expression. As already mentioned, the discrete lifting operator G_{lifted} is a transfer function matrix with dimensions $N_y \times N_u$, and so it is the complex-valued frequency response $\overline{G}_{lifted}(e^{j\omega T_0})$, being, as previously mentioned, T_0 the least common multiple of input T_u and output T_y periods.

In order to evaluate the gain of this frequency response matrix, the induced 2-norm may be used as in the *sigma plots* of conventional multivariable systems. That is, the maximum gain of the frequency response at a particular frequency of a dual-rate system may be considered to be:

$$\|\overline{G}_{lifted}(e^{j\omega T_0})\|_2 = \overline{\sigma}[\overline{G}_{lifted}(e^{j\omega T_0})] \quad (4)$$

i.e., the maximum singular value $\overline{\sigma}$ of the discrete lifting transfer matrix, for each frequency. However, such frequency response is only evaluated at the slow rate (meta-period) $T_0 = NT$ and, hence, the nuances of possible resonances, ripples, etc. at faster frequences cannot be extracted because of aliasing at frequencies larger than π/T_0. This motivates the present work.

Turning back to the original computations to sinusoidal signals (under the assumption that the frequency response is not computed at locations of unit-circle poles), the following may be stated:

Theorem 1 *The output $y(k)$, when $u(k) = e^{j\omega T_u k}$, of a SISO dual-rate ($N_u T_u = N_y T_y$) lifted system $y_l(z) = G_{lifted}(z)u_l(z)$ is a collection of components $y_r(k) = \bar{y}_r e^{jT_y\omega_r k}$ of frequencies $\omega_r = \omega + 2\omega_y^s r/N_y$, for $r = 0, \ldots, (N_y - 1)$, with $\omega_y^s = \pi/T_y$, and $\bar{y}_r$ is given by:*

$$\bar{y}_r = \frac{1}{N_y} \sum_{p=0}^{N_y-1} \sum_{q=0}^{N_u-1} G_{pq}(e^{j\omega_r T_y N_y}) e^{-jT_y\omega_r p} e^{j\omega T_u q} \tag{5}$$

Proof: Let the lifted system be $y_l(z) = G_{lifted}(z)u_l(z)$, and denote elements of G_{lifted} as G_{pq} ($p = 0, \ldots, N_y - 1$; $q = 0, \ldots, N_u - 1$).

Consider the input signal $u(k) = e^{j\omega T_u k}$. When lifted to a $N_u \times 1$ vector, the q-th element ($q = 0, \ldots, N_u - 1$) of sample k will be

$$e^{j\omega T_u(N_u k+q)} = e^{j\omega N_u T_u(k+q/N_u)} = \left(e^{j\omega N_u T_u}\right)^k e^{j\omega T_u q}$$

Hence, the stationary sequence for output p will be:

$$y_{l,p}(k) = \sum_{q=0}^{N_u-1} G_{pq}(e^{j\omega N_u T_u}) e^{j\omega T_u q} \left(e^{j\omega N_u T_u}\right)^k \tag{6}$$

When undoing the lifting, the p-th element of $y_l(k)$, *i.e.*, $y_{l,p}(k)$ must appear at time $(kN_y + p)T_y$ in the non-lifted sequence, *i.e.*, at positions p, $p + N_y$, $p + 2N_y$, ... By using t_k in (3) we may write that the elements at positions $k = 0, N_y, 2N_y, \ldots$ are given by $t_k y_{l,0}(k/N_y)$. Those at positions $k = 1, N_y + 1, 2N_y + 1, \ldots$ are given by delaying one sample the sequence $t_k y_{l,1}(k/N_y)$, *i.e.*, the expression: $t_{k-1} y_{l,1}((k-1)/N_y)$, and so on. Adding all

the sequences, we have[2]:

$$y(k) = \sum_{p=0}^{N_y-1} t_{k-p} \cdot y_{l,p}\left((k-p)/N_y\right) \tag{7}$$

Hence, replacing (6) in (7), we obtain:

$$y(k) = \sum_{p=0}^{N_y-1} t_{k-p} \sum_{q=0}^{N_u-1} G_{pq}(e^{j\omega N_u T_u}) e^{j\omega T_u q} \left(e^{j\omega \frac{N_u T_u}{N_y}}\right)^{k-p} \tag{8}$$

so that, using $N_u T_u = N_y T_y$ and (3), we get $y(k)$ to be:

$$\sum_{p=0}^{N_y-1} \sum_{r=0}^{N_y-1} \frac{e^{j\frac{2\pi r(k-p)}{N_y}}}{N_y} \sum_{q=0}^{N_u-1} G_{pq}(e^{j\omega N_u T_u}) e^{j\omega T_u q} e^{j\omega T_y (k-p)}$$

Rearranging terms to recover the components:

$$y(k) = \sum_{r=0}^{N_y-1} \Xi_r(\omega) \left(e^{j(\omega T_y + \frac{2\pi r}{N_y})}\right)^k \tag{9}$$

where the component Ξ_r is given by:

$$\Xi_r(\omega) = \frac{1}{N_y} \sum_{p=0}^{N_y-1} \sum_{q=0}^{N_u-1} G_{pq}(e^{j\omega N_u T_u}) e^{j\omega T_u q} e^{-j(\omega T_y + \frac{2\pi r}{N_y})p}$$

Denoting $\omega_y^s = \pi/T_y$, and also taking into account that

$$e^{j\omega N_u T_u} = e^{j(\omega + 2r\pi/(N_y T_y))N_y T_y} = e^{j\omega_r T_y N_y} \tag{10}$$

we have the result stated in the theorem. □

The above result may be easily extended to a multivariable case in which G_{pq} is a matrix, by considering the input to be $u(k) = \upsilon e^{j\omega T_u k}$ being υ an arbitrary convex-valued vector indicating the amplitudes and phase shifts of each input (details omitted for brevity).

[2]Note that a slight abuse of notation has been used in (7): any arbitrary finite value may be assigned to $y_{l,p}(\psi)$ for non-integer ψ because when multiplied by t_{k-p} it will, anyway, be zero. It will be non-zero only when $\psi = (k-p)/N_y$ is an integer and so $k-p$ is multiple of N_y.

3.1. Relationship to classic frequency-response computations

Discrete frequency-response computations in mainstream control software are carried out by replacing $z = e^{j\omega T}$ for some T. It is easy to chech that, from (5), the components will be given by the product of the frequency response of a left factor:

$$[1 \; z^{-1} \; z^{-2} \; \ldots \; z^{-(N_y-1)}]G_{lifted}(z^{N_y})$$

replacing $z = e^{j\omega_r T_y}$, which gives a row vector, and the right factor (column vector)

$$(1 \; z \; z^2 \; \ldots z^{N_u-1})^T$$

replacing $z = e^{j\omega T_u}$. In a MIMO case, the left factor would be

$$[I_y \; z^{-1}I_y \; \ldots \; z^{-(N_y-1)}I_y]G_{lifted}(z^{N_y})$$

, and the right one $(I_u \; zI_u \; \ldots z^{N_u-1}I_u)^T$, where I_y is the $N_y \times N_y$ identity matrix and I_u is the $N_u \times N_u$ one. This is not, in general, an ordinary frequency response computation because two different substitutions for z are needed.

In the particular case of $N_u = 1$, the right factor becomes equal to 1, so the components can be computed as the usual frequency response of the left factor with period T_y. In the case $N_y = 1$, the single component can be obtained by plotting the frequency response of:

$$G_{lifted}(z^{N_u})(1 \; z \; z^2 \; \ldots z^{N_u-1})^T \tag{11}$$

at period T_u (note that, from (10), $e^{j\omega_r T_y N_y} = e^{j\omega T_u N_u}$).

3.2. Coprime case

There is the possibility of computing the whole frequency response from only one Bode plot in the case N_y and N_u are coprime. Denote $\omega_s = 2\pi/(N_y T_y)$.

Then, the components of the frequency response are $\omega_r = \omega + r\omega_s$.

Indeed, from (5), any of the terms $e^{j\omega T_u q}$ can be replaced by $e^{j\omega T_u q + 2\pi k_u q} = e^{j(\omega + \omega_s k_u N_u)T_u q}$, for any integer k_u. Similarly, for any integer k_y, the terms $e^{-j\omega_r T_y p}$ can be replaced by$e^{-j(\omega + r\omega_s + k_y \omega_s N_y)T_y p}$. Hence, if there exists ω^*, k_u, k_y so that:

$$\omega^* = \omega + r\omega_s + k_y \omega_s N_y = \omega + \omega_s k_u N_u \tag{12}$$

then expression (5) can be computed as:

$$\bar{y}_r = \frac{1}{N_y} \sum_{p=0}^{N_y-1} \sum_{q=0}^{N_u-1} G_{pq}(e^{j\omega^* T_y N_y}) e^{-jT_y\omega^* p} e^{j\omega^* T_u q} \tag{13}$$

Note that (12) holds if and only if:

$$r = k_u N_u - k_y N_y \tag{14}$$

The above equation is a well-known diophantine equation in the integer ring, which has a solution for any r if N_u and N_y are coprime so that, finding a particular solution k_u^*, k_y^* for the Bezout identity:

$$1 = k_u^* N_u - k_y^* N_y \tag{15}$$

all solutions of (14) are, for any arbitrary integer p:

$$k_u = k_u^* r + N_y p$$

hence:

$$\omega^* = \omega + k_u^* r * N_u \omega_s + p N_y N_u \omega_s \tag{16}$$

Based on the above, theorem 1 can be restated as:

Theorem 2 *The output $y(k)$, when $u(k) = e^{j\omega T_u k}$, of a SISO dual-rate ($N_u T_u = N_y T_y$) lifted system $y_l(z) = G_{lifted}(z) u_l(z)$ is a collection of components $y_r(k) = \bar{y}_r e^{jT_y \omega_r k}$ of frequencies $\omega_r = \omega + \omega_s r$, for $r = 0, \ldots, (N_y - 1)$. Denoting by $T_{min} = T_u/N_y = T_y/N_u$, $\bar{y}_r$ is given by the result of evaluating at $z = e^{jT_{min}\omega^*}$ the matrix expression:*

$$(1 \;\; z^{-N_u} \;\; \ldots z^{-(N_y-1)N_u}) \frac{G_{lifted}(z^{N_y N_u})}{N_y} \begin{pmatrix} 1 \\ z^{N_y} \\ \vdots \\ z^{(N_u-1)N_y} \end{pmatrix} \tag{17}$$

where ω^* is computed following the Diophantine equation approach above.

Note that the above result is *not* valid if N_u and N_y are not coprime.

Example. For $N_y = 3$, $N_u = 2$, the Bezout equation admits a solution $k_u^* = 2$,$k_y^* = 1$. Hence, the components of the frequency response will be read in the above transfer function at frequencies:

$$(r = 0) : \omega, \;\; (r = 1) : \omega + 4\omega_s, \;\; (r = 2) : \omega + 2\omega_s$$

3.3. Bezout tables

In the previous example, the associated Bezout equation is closely related to the table below:

m	0	1	2	0	1	2
n	0	1	0	1	0	1
k	0	1	2	3	4	5

(18)

which can be interpreted in the following terms: when the input is a sinusoidal of frequency $\omega + n\omega_s$, the output component of frequency $\omega + m\omega_s$ is given by the ordinary frequency response of (17) at $\omega + k\omega_s$.

Proof is evident by using an input frequency $\omega + n\omega_s$ instead of ω and $m = r + n$ in Theorem 2 and, then, realising that $k_u^* N_u$ is obtained at the position $m = 1$, $n = 0$. Indeed, (15) means that one plus k_y times counting N_y numbers must be equal to counting N_u integers a total of k_u times, which is what the table does.

As another example, for $N_y = 4$, $N_u = 3$ we would have a Bezout table:

m	0	1	2	3	0	1	2	3	0	1	2	3
n	0	1	2	0	1	2	0	1	2	0	1	2
k	0	1	2	3	4	5	6	7	8	9	10	11

(19)

as, indeed, the solution to the Bezout equation, i.e., $1 = 3N_u - 2N_y$, is found at $k = 9$ in the table. So, the three output harmonics when u has a frequency $\omega \in [0, \omega_s)$ would be found by reading the Bode diagram of (17) at $\omega + 9\omega_s$, at $\omega + 6\omega_s$ and at $\omega + 3\omega_s$. When u has a frequency $\omega \in [1, 2)\omega_s$, the output component in $[0, \omega_s)$ would be read at $\omega + 4\omega_s$, that in in $[1, 2)\omega_s$ would be read at $\omega + \omega_s$, the component in $[2, 3)\omega_s$ would be read at $\omega + 10\omega_s$, and the last component in $[3, 4)\omega_s$ would be read at $\omega + 7\omega_s$.

3.4. Multi-sine input (system interconnection)

As the output of a dual-rate system when subject to a sinusoidal input is a combination of sinusoidal components, in general, the response of a cascaded or closed-loop system to such a combination of input components will be obtained by means of the superposition principle and application of previous results.

Let us consider the input to be:

$$u_k = \sum_{n=0}^{N_u - 1} c_n e^{j(\omega + n\omega_s)T_u k} \tag{20}$$

with $\omega \in [0, \omega_s)$. Denote with $\omega_n = \omega + n\omega_s$.

Theorem 3 *The output $y(k)$, when $u(k)$ is given by* (20)*, of a SISO dual-rate ($N_u T_u = N_y T_y$) lifted system $y_l(z) = G_{lifted}(z)u_l(z)$ is a collection of components $y_r(k) = \bar{y}_r e^{jT_y\omega_r k}$ of frequencies $\omega_r = \omega + \omega_s r$, for $r = 0, \ldots, (N_y - 1)$, with $\omega_s = 2\pi/(N_y T_y)$, and $\bar{y}_r$ is given by:*

$$\bar{y}_r = \frac{1}{N_y} \sum_{n=0}^{N_u-1} \sum_{p=0}^{N_y-1} \sum_{q=0}^{N_u-1} G_{pq}(e^{j\omega T_y N_y}) e^{-jT_y\omega_r p} c_n e^{j\omega_n T_u q} \tag{21}$$

The proof has no difficulty from previous results and superposition, as above commented.

In the coprime case, given that all terms in the frequency response can be computed from that of a single transfer function, we have the following practical result:

Theorem 4 *The output component at frequency $\omega + m\omega_s$ is given by the m-th component of the vector (starting index equal to zero) C_y given by:*

$$\psi = G_{FR} C_u \tag{22}$$

where C_u is a column vector which contains the input components c_n, and G_{FR} is a $N_y \times N_u$ frequency response matrix whose element m, n is given by $G_B(\omega + k\omega_s)$, where G_B is the result of (17)*, and k is obtained from the Bezout table.*

Example. In the case $N_y = 4$, $N_u = 3$, from the Bezout table in previous examples, denoting $\omega_k = \omega + k\omega_s$ the frequency response matrix will be given by:

$$\begin{pmatrix} G_B(\omega_0) & G_B(\omega_4) & G_B(\omega_8) \\ G_B(\omega_9) & G_B(\omega_1) & G_B(\omega_5) \\ G_B(\omega_6) & G_B(\omega_{10}) & G_B(\omega_2) \\ G_B(\omega_3) & G_B(\omega_7) & G_B(\omega_{11}) \end{pmatrix} \tag{23}$$

4. Examples of computation of frequency response

Example 1. In [34], an example on a continuous-time system with transfer function $G_c(s) = 1/(s^2 + s + 2)$ ZOH-discretised at $T = 0.2$ seconds, with $N_u = N_y = 3$ shows that Theorem 1 actually discovers that such sampling

pattern is a "conventional" sampling disguised as a multirate one. So, the AC representation results (see reference for details), as expected, in:

$$\begin{pmatrix} G(e^{j\omega T}) & 0 & 0 \\ 0 & G(e^{j(\omega+\omega_s)T}) & 0 \\ 0 & 0 & G(e^{j(\omega+2\omega_s)T}) \end{pmatrix} \tag{24}$$

Example 2. For the same continous-time plant as in the previous example, consider a realization of an auxiliary ZOH discretisation at $T = 0.1$ seconds, with matrices A, B, C, $D = 0$. Denote $B^h = (A+I)B$. Setting $N_u = 3$, $T_u = 0.2$, $N_y = 2$, $T_y = 0.3$, and metaperiod $T_0 = NT$, being $N = lcm(N_u, N_y)$ and $T = gcd(T_u, T_y)$, the following dual-rate lifted model is obtained:

$$\begin{array}{rcl} x(k+1) & = & A^6 x(k) + (A^4B^h \;\; A^2B^h \;\; B^h)u_l(k) \\ y_l(k) & = & \begin{pmatrix} C \\ CA^3 \end{pmatrix} x(k) + \begin{pmatrix} 0 & 0 & 0 \\ CAB^h & CB & 0 \end{pmatrix} u_l(k) \end{array} \tag{25}$$

Computing its transfer function, we have a left factor for Theorem 1 $Q(z) = (1 \; z^{-3})\frac{1}{2}G_{lift}(z^6)$, and a right factor $(1 \; z^2 \; z^4)^T$. Setting, for instance, $\omega = 4$, the obtained components are $-0.0664 + 0.00811i$ for the fundamental component (4 rad/s) and $0.0000911 - 0.0000489i$ for the second one ($4+\pi/0.3$ rad/s). In order to check the results, the actual time response will be computed. Consider the lifted input sequence:

$$u_l(k) = (\cos(\omega T_0 k) \;\; \cos(\omega T_0 k + \omega T_u) \;\; \cos(\omega T_0 k + 2\omega T_u))^T$$

Transformed to Z-domain, for $\omega = 4$, we get:

$$u_l(z) = \frac{1}{z^2 - 2\cos\left(\frac{12}{5}\right) z + 1} \begin{pmatrix} z\left(z - \cos\left(\frac{12}{5}\right)\right) \\ z\left(z\cos\left(\frac{4}{5}\right) - \cos\left(\frac{8}{5}\right)\right) \\ z\left(z\cos\left(\frac{8}{5}\right) - \cos\left(\frac{4}{5}\right)\right) \end{pmatrix}$$

The discrete lifting operator is the transfer function matrix from (25).

Then, the lifted output sequence is $y_l(z) = G_{lifted}(z)u_l(z)$, and the actual output one (reversing the lifting operator) is: $(1 \; z^{-1})y(z^2)$ where an expand operator ($z \mapsto z^2$) has been applied prior to multiplication. The resulting inverse Z-transform $y(k)$ is a transient regime (decaying to zero):

$$\begin{aligned} y_{trans}(k) = (0.03313 + 0.02681i)(0.793812 - 0.332687i)^k + \\ + (0.03313 - 0.02681i)(0.793812 + 0.332687i)^k \end{aligned}$$

plus a steady-state frequency response with two components given by:

$$\begin{aligned} y_{steady}(k) = (0.00004583 - 0.0000245i)(-0.362358 - 0.932039i)^k + \\ + (0.00004583 + 0.0000245i)(-0.362358 + 0.932039i)^k - \\ - (0.03318 + 0.004057i)(0.362358 - 0.932039i)^k - \\ - (0.03318 - 0.004057i)(0.362358 + 0.932039i)^k \end{aligned}$$

corresponding to $e^{\pm j4T_y} = (-0.362358 \pm 0.932039i)$ and $e^{\pm j4T_y + \pi} = (0.362358 \pm 0.932039i)$, i.e., the two frequency components (4 rad/s and $(4 + \pi/0.3) = 14.472$ rad/s, respectively). The coefficients associated to those terms correspond to the results of Theorem 1, taking into account the fact that $\cos(\omega T) = 0.5(e^{j\omega T} + e^{-j\omega T})$ and round-off numerical errors.

Example 3. If $N_y = 3$, $N_u = 2$ is chosen and a lifted model is suitably generated from the realisation of the ZOH discretization at $T = 0.1$, application of Theorem 1 for different frequencies results in the frequency plot (generalized Bode diagram) in Figure 1: at low frequencies, the non-fundamental components have a negligible amplitude and the response is, basically, the same as the conventionally-sampled single-rate system at $T_u = 0.3$. Indeed, at very low frequencies, the plant output is basically constant.

In order to check Theorem 2, the Bode diagram of the conventionally-sampled system generated from (17), i.e.:

$$\frac{0.00161z^3 + 0.003167z^2 + 0.003167z + 0.001557}{z^4 - 1.886z^3 + 0.9048z^2}$$

is depicted in Figure 2. It can be seen that the components in the conventional Bode diagram in Figure 2 are, indeed, portions of the diagram in Figure 1 (in order to suitably compare the figures, note that all axis are in logarithmic scale).

5. Application: Multirate Control Design Ripple Frequency Detection and Suppression

In this section an example leads to explain the advantages of using the methodology exposed before. Consider the plant to be controlled:

$$G_p(s) = \frac{1.5}{(s + 0.5)(s + 1.5)} \tag{26}$$

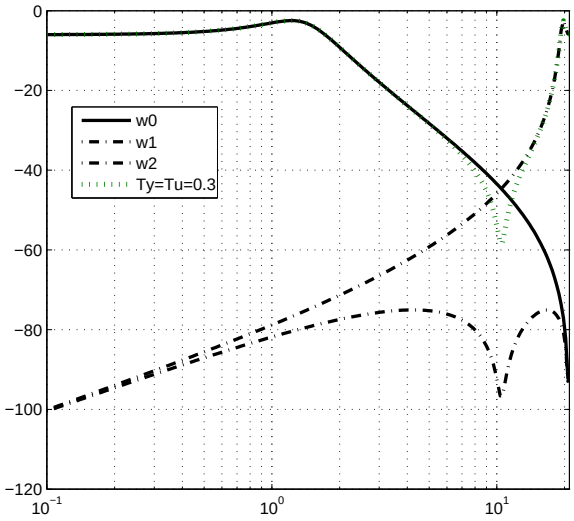

Figure 1: Generalized dual-rate Bode diagram ($T_u = 0.3$,$T_y = 0.2$), depicting induced components (at frequency ω in the abscissae axis there appear the amplitude of components at frequency w, $w + 2\pi/(0.2 \cdot 3)$, $w + 4\pi/(0.2 \cdot 3)$). For comparison, the frequency response of the system with conventional sampling at $T_u = 0.3s$ is presented in dotted-green line.

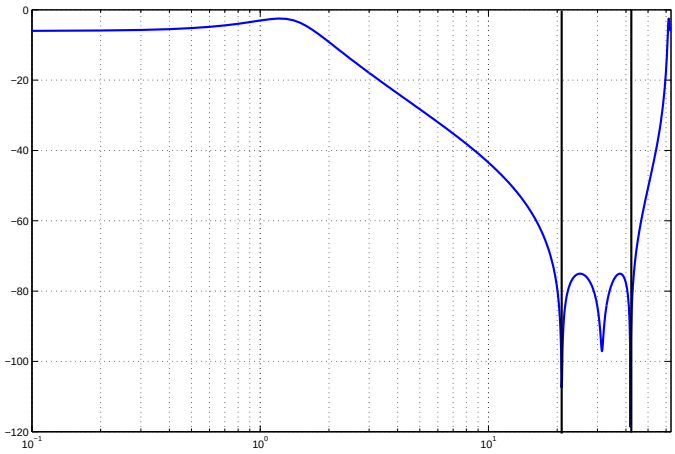

Figure 2: Dual-rate Bode diagram ($T_u = 0.3$,$T_y = 0.2$), depicting the harmonics in Fig. 1 (Coprime Case: single TF)

A suitable temporal behavior in the continuous response of the plant called $M(s)$ will be found by using a convenient PID continuous regulator; for example:

$$G_R(s) = K_p[1 + T_d s + \frac{1}{T_i s}] \tag{27}$$

with $K_p = 8$, $T_d = 0.2s.$, and $T_i = 3.2s$. This regulator will be discretised with, for instante, the discretisation in [37]:

$$G_R(z) = \frac{q_0 + q_1 z^{-1} + q_2 z^{-2}}{1 - z^{-1}} \tag{28}$$

with parameters defined by

$$\begin{array}{l} q_0 = K_p(1 + \frac{T_d}{T}) \\ q_1 = -K_p(1 + 2\frac{T_d}{T} - \frac{T}{T_i}) \\ q_2 = K_p(\frac{T_d}{T}) \end{array} \tag{29}$$

As the sampling period increases, the performance of the loop decreases. It is reasonably close to the continous-time one for $T \leq 0.2$, it degrades quite a lot for $T \geq 0.4$ and, in fact, it gets unstable for $T \approx 0.5$.

Of course, the regulator can be designed taking this scarcer sampling into account but, as discussed in [35], dual-rate schemes can extend the validity of discretization-based designs for longer periods. As the objective of the paper is not designing optimal-performance controllers but using the dual-rate frequency response tools to detect potential problems in the loops, the redesign of the controller departing from the discretised PID framework will be pursued no further.

So, taking the PID again, we will assume that, for some reason, it is not possible to take samples of the output process with period smaller than $0.4s$, but we will also assume that it is possible to design a dual-rate regulator that operates with sampling intervals $T_y = 0.4$ s and $T_u = 0.4/3$ s in the output and input, respectively. So let us choose the setting $NT = 0.4$ s, $N_y = 1$, $N_u = 3$.

In the work developed by [35] and according to the scheme shown in Figure 3, the sub-regulators equations will be found by means of

$$\begin{array}{l} G_{Rslow}(z_{sl}) = \frac{1}{1 - M(z_{sl})} \\ G_{Rfast}(z_{fs}) = \frac{M(z_{fs})}{G(z_{fs})} \end{array} \tag{30}$$

where:

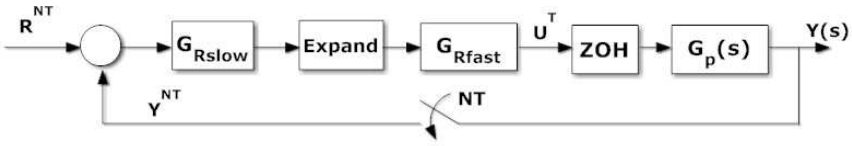

Figure 3: Dual-Rate Control Scheme

- The z variables z_{sl} and z_{fs} are related to slow and fast periods respectively $T_{sl} = T_y = NT$ and $T_{fs} = T_u$,
- In the same way $M(z_{sl})$ and $M(z_{fs})$ represents the desired behavior of the closed loop system $M(s)$ discretized with zero order hold to T_{sl} and T_{fs} respectively [3]. $G(z_{fs})$ will be the ZOH-discretization of the plant at the fast rate.

In the simulation, the output is found that follows $M(s)$ perfectly but shows a ripple between samples at a frequency of

$$w_{ripple} = \frac{2\pi}{T_{ripple}} = \frac{2\pi}{0.266} \cong 23.6 Rad/s \tag{31}$$

In the reference [35], an alternative method in order to avoid this problem is introduced. All of the above can be observed in plots in Figure 4, in the time domain.

The objective of this example is to show that the frequency computation tool developed here is able to observe these different behaviours at the correct frequencies instead of at the "aliased" ones arising from considering only the slow-rate meta-period.

Figures 5 and 6 (detail) show the generalised Bode diagram of two different control strategies, as well as the maximum singular value plot of the low-rate lifted representation for comparison.

The frequency response curve of the closed loop system with the dual-rate regulator obtained like in [35], shows the oscillating behavior between samples with the presentation of a significant response peak in the area of close to the slow-rate Nyquist frequency. This results in aliasing which conceals such peak in such a way that it is barely distinghishable in the singular-value lifted

[3] For simplicity a stable and minimum phase system will be assumed. There is a valid procedure in those cases. See [38]

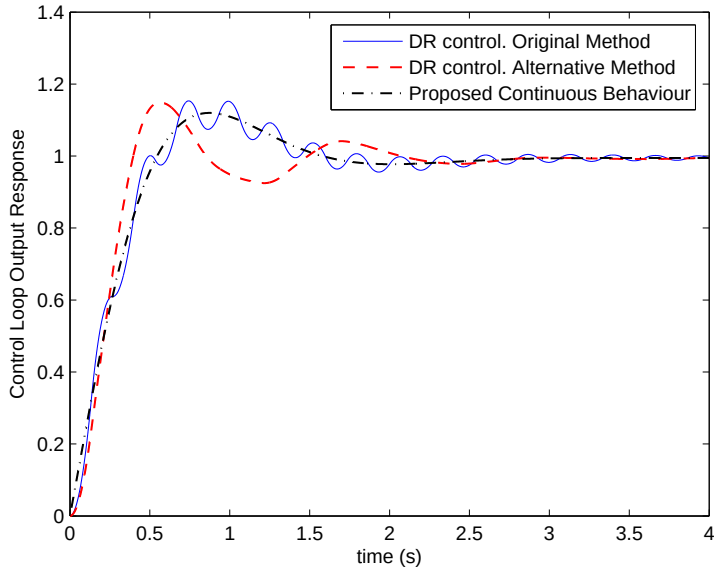

Figure 4: Dual-Rate Control. Unit step response

diagram. Also, the peak is detected at several higher-frequency aliases. From the svd lifted diagram it is not possible to truly apprehend the actual ripple frequency and its amplitude. However, with the generalised Bode diagram, the ripple amplitude and frequency are clearly depiced. Hence, the proposals in this paper seem to be better suited for analysing this kind of problems than the sigma-plot of the lifted plant.

Following with the example, an attempt will be made to diminish the magnitude of the response peak causing the oscillatory behavior by applying a discrete-time *single notch* filter in the form of

$$F(z_{fs}) = 0.72\frac{z_{fs} + 0.995}{z_{fs} + 0.4} \tag{32}$$

operating at a period T_{fs}. With this filter one zero next to the Nyquist frequency is introduced in order to cancel the ripple on the dual-rate scheme. Some reasonable dynamic is added an then the gain is adjusted. This behavior of selective rejection, shown in Figure 7, produce the elimination of the undesired intersample ripple while maintaining the other frequency domain characteristics of the system relatively unchanged. See figures 7 and 8 for frequency and time-domain results.

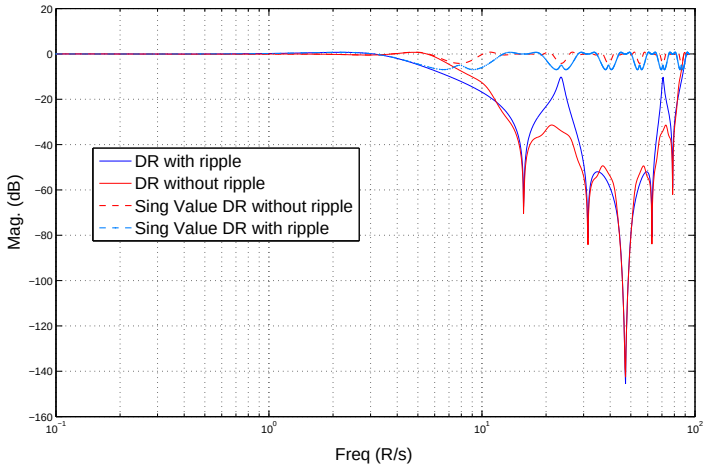

Figure 5: Frequency Response and maximum singular values

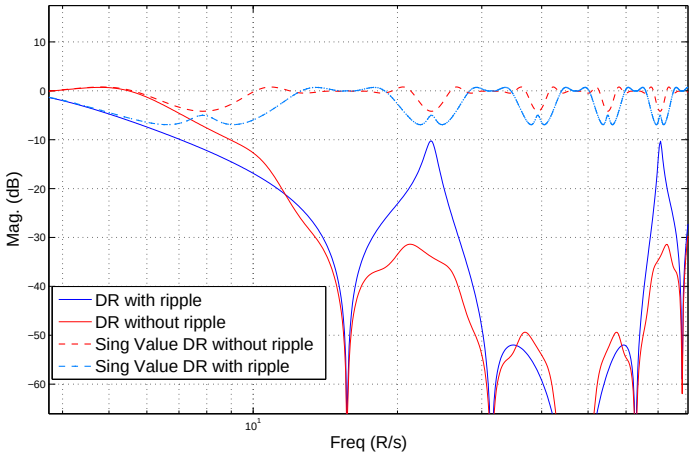

Figure 6: Frequency Response and maximum singular values: Zoom

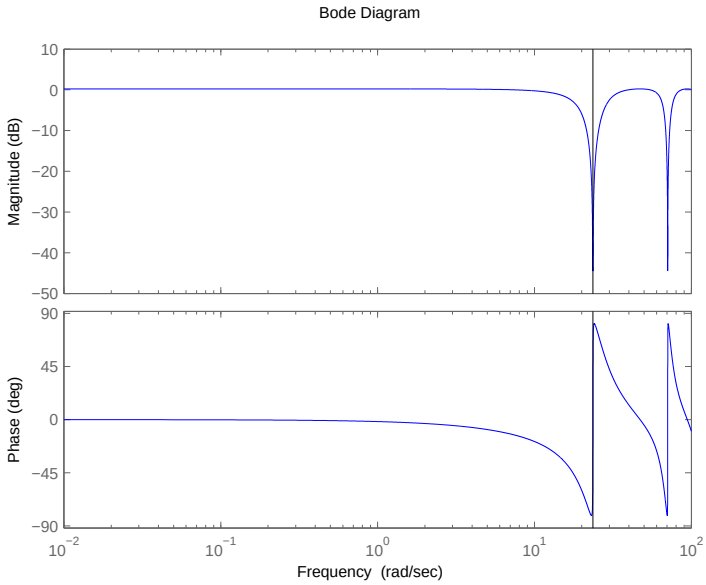

Figure 7: Filter $F(z_{fs})$ frequency response

As previously discussed, the generalised frequency-response diagram clearly shows how the notch elliminates the ripple, and there is no aliasing to disguise at which frequencies and amplitudes the filter effect is present.

Finally, the time response to the unit step when this compensating notch filter is added is now presented; see results in Figure 9.

6. Conclusions

The output of a dual-rate sampled system is a sum of component sinusoids when the input is a discrete sinuosidal input. An easy way to compute this frequency response of a dual-rate system is presented in this paper completing previous preliminary work by the authors. The procedure leads to a generalised Bode diagram; in the case of coprime input-ouput sampling periods a conventional Bode diagram (suitably rearranged) can describe all components of the system response. The different frequency components can be arranged on a table arising from Bezout's identities and lifting procedures. The techniques are applied to dual-rate automatic feedback control problems; they lead to an exact procedure useful to detect and overcome

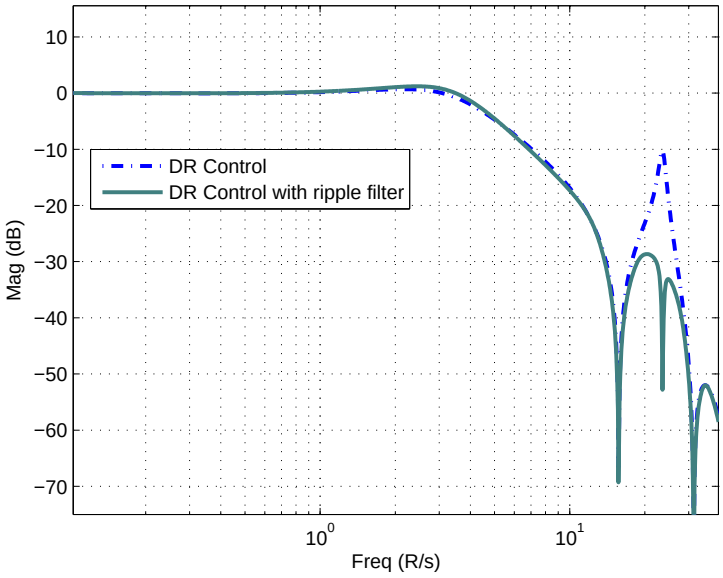

Figure 8: Time response to the unit step. System with dual rate regulator in dotted line, and system with DR control compensated by $F(z_{fs})$ in bold solid.

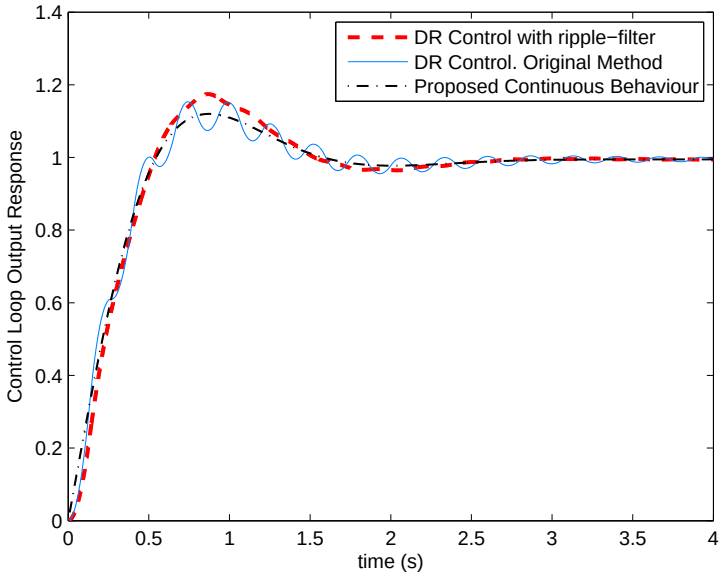

Figure 9: Close Loop Time Response. Ripple suppressed

ripple phenomena in that kind of systems. This overcomes some conservativeness issues from using a multivariable frequency-response (singular value) description of single-rate lifted systems in literature: such approach leaves out specific properties of the multirate systems wich are kept in the proposed methodology.

7. References

[1] P. Khargonekar, K. Poolla, A. Tannenbaum, Robust control of linear time-invariant plants using periodic compensation, Automatic Control, IEEE Transactions on 30 (11) (1985) 1088–1096.

[2] B. Francis, T. Georgiou, Stability theory for linear time-invariant plants with periodic digital controllers, Automatic Control, IEEE Transactions on 33 (9) (1988) 820–832.

[3] J. Tsai, C. Wang, C. Kuang, S. Guo, L. Shieh, C. Chen, A NARMAX model-based state-space self-tuning control for nonlinear stochastic hybrid systems, Applied Mathematical Modelling 34 (10) (2010) 3030–3054.

[4] R. Whalley, Multidimensional systems and multirate sampling, Applied Mathematical Modelling 14 (3) (1990) 132–139.

[5] P. Albertos, A. Crespo, Real-time control of non-uniformly sampled systems, Control Engineering Practice 7 (4) (1999) 445–458.

[6] V. Joshi, L. Xie, J. Park, L. Shieh, Y. Chen, K. Grigoriadis, J. Tsai, Digital modeling and control of multiple time-delayed distributed power grid, Applied Mathematical Modelling 36 (9) (2011) 4118–4134.

[7] Á. Cuenca, J. Salt, A. Sala, R. Pizá, A delay-dependent dual-rate pid controller over an ethernet network, Industrial Informatics, IEEE Transactions on 7 (1) (2011) 18–29.

[8] J. Ding, F. Marcassa, S. Wu, M. Tomizuka, Multirate control for computation saving, Control Systems Technology, IEEE Transactions on 14 (1) (2006) 165–169.

[9] P. Kabamba, Control of linear systems using generalized sampled-data hold functions, Automatic Control, IEEE Transactions on 32 (9) (1987) 772–783.

[10] J. Tsai, C. Chen, L. Shieh, Modelling of multirate feedback systems using uniform-rate models, Applied mathematical modelling 17 (1) (1993) 2–14.

[11] M. Cimino, P. Pagilla, Design of linear time-invariant controllers for multirate systems, Automatica 46 (8) (2010) 1315–1319.

[12] M. Cimino, P. Pagilla, Conditions for the ripple-free response of multirate systems using linear time-invariant controllers, Systems & Control Letters 59 (8) (2010) 510–516.

[13] Y. Du, J. Tsai, H. Patil, L. Shieh, Y. Chen, Indirect identification of continuous-time delay systems from step responses, Applied Mathematical Modelling 35 (2) (2011) 594–611.

[14] B. Friedland, Sampled Data Control Systems Containing Periodically Varying Numbers, United States Air Force, Office of Scientific Research, 1959.

[15] B. Bamieh, J. Pearson, B. Francis, A. Tannenbaum, A lifting technique for linear periodic systems with applications to sampled-data control, Systems & Control Letters 17 (2) (1991) 79–88.

[16] F. D. T. Chen, Hierarchical identification of lifted state-space models for general dual-rate systems, Circuits and Systems I: Regular Papers, IEEE Transactions on [Circuits and Systems I: Fundamental Theory and Applications, IEEE Transactions on] 52 (6) (June 2005) 1179–1187. doi:10.1109/TCSI.2005.849144.

[17] P. Albertos, Block multirate input-output model for sampled-data control systems, Automatic Control, IEEE Transactions on 35 (9) (1990) 1085–1088.

[18] R. Meyer, C. Burrus, A unified analysis of multirate and periodically time-varying digital filters, Circuits and Systems, IEEE Transactions on 22 (3) (1975) 162–168.

[19] G. Kranc, Input-output analysis of multirate feedback systems, Automatic Control, IRE Transactions on 3 (1) (1957) 21–28.

[20] P. Vaidyanathan, Multirate systems and filter banks, 1993.

[21] T. Chen, B. Francis, Optimal sampled-data control systems, Vol. 124, Springer London, 1995.

[22] J. Li, R. Ding, Y. Yang, Iterative parameter identification methods for nonlinear functions, Applied Mathematical Modelling 36 (6) (2012) 2739–2750.

[23] L. Zhuang, F. Pan, F. Ding, Parameter and state estimation algorithm for single-input single-output linear systems using the canonical state space models, Applied Mathematical Modelling 36 (8) (2012) 3454–3463.

[24] Y. Gua, F. Dingb, Auxiliary model based least squares identification method for a state space model with a unit time-delay, Applied Mathematical Modelling 36 (12) (2012) 5773–5779.

[25] J. Ding, C. Fan, J. Lin, Auxiliary model based parameter estimation for dual-rate output error systems with colored noise, Applied Mathematical Modelling.

[26] L. Chai, L. Qiu, Topics on multirate systems: frequency response, interpolation, model validation, in: Decision and Control, 2000. Proceedings of the 39th IEEE Conference on, Vol. 5, IEEE, 2000, pp. 4290–4295.

[27] G. Goodwin, A. Feuer, S. Lee, On the reconstruction of a finite sum of sinusoids from non-uniform periodic samples, International Journal of Control 71 (4) (1998) 615–629.

[28] P. Sarhadi, K. Salahshoor, A. Khaki-Sedigh, Robustness analysis and tuning of generalized predictive control using frequency domain approaches, Applied Mathematical Modelling 36 (12) (2012) 6167–6185.

[29] M. Sayed, M. Kamel, Stability study and control of helicopter blade flapping vibrations, Applied Mathematical Modelling 35 (6) (2011) 2820–2837.

[30] R. Shenoy, Multirate specifications via alias-component matrices, Circuits and Systems II: Analog and Digital Signal Processing, IEEE Transactions on 45 (3) (1998) 314–320.

[31] A. Mehr, Alias-component matrices of multirate systems, Circuits and Systems II: Express Briefs, IEEE Transactions on 56 (6) (2009) 489–493.

[32] M. Araki, K. Yamamoto, Multivariable multirate sampled-data systems: state-space description, transfer characteristics, and nyquist criterion, Automatic Control, IEEE Transactions on 31 (2) (1986) 145–154.

[33] J. Salt, J. Sandoval, P. Albertos, Dual-Rate Control Ripple Detection by an Approximate Frequency Response Methodology, Electronics, Robotics and Automotive Mechanics Conference, 2007. CERMA 2007 (2007) 89–94.

[34] A. Sala, J. Salt, J. Sandoval, Frequency response of discrete dual-rate systems, in: Advanced Engineering Computing and Applications in Sciences, 2008. ADVCOMP'08. The Second International Conference on, IEEE, 2008, pp. 129–134.

[35] J. Salt, P. Albertos, Model-Based Multirate Controllers Design, Control Systems Technology, IEEE Transactions on 13 (6) (2005) 988–997.

[36] J. Salt, J. Torneno, P. Albertos, Modelling of non-conventional sampled data systems, Control Applications, 1993., Second IEEE Conference on (1993) 631–635.

[37] I. Rolf, Digital control systems (1981).

[38] J. Salt, A. Sala, P. Albertos, A transfer-function approach to dual-rate controller design for unstable and non-minimum-phase plants, Control Systems Technology, IEEE Transactions on 19 (5) (2011) 1186–1194.